ORIGINAL PAPER: SOL-GEL, HYBRIDS AND SOLUTION CHEMISTRIES

CrossMark

Novel route to synthesize CaAl- and MgAl-layered double hydroxides with highly regular morphology
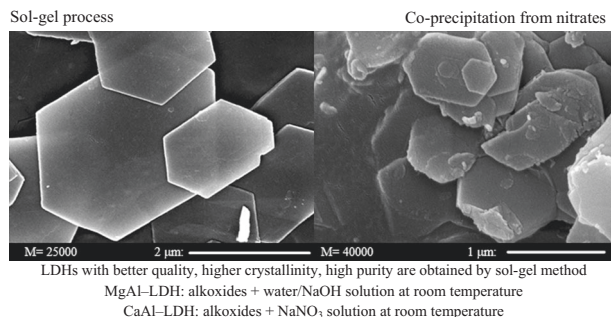
Szabolcs Muráth[1,2] · Zoltán Somosi[1,2] · Ákos Kukovecz[3] · Zoltán Kónya[3,4] · Pál Sipos[2,5] · István Pálinkó [1,2]

Abstract

A facile, sol–gel method was developed to obtain Al-containing layered double hydroxides (LDHs) with Ca or Mg divalent cations. Ca- and Al-alkoxide were added to aqueous $NaNO_3$ solution, and, after rapid gelation, a solid product, phase-pure, highly crystalline CaAl–LDH was formed with exceptionally regular morphology without impurities for the first time with sol–gel method. The lack of salt in the solution used for the hydrolysis resulted in a non-desirable by-product (katoite). For the sol–gel synthesis of MgAl–LDH, it was found that its formation was less sensitive to the presence of nitrate ions, and pure water or aqueous NaOH worked equally well. The product was also a highly crystalline material with thin, plate-like morphology as revealed by X-ray diffractometry and scanning electron microscopy. IR measurements indicate the lack of organic substance in the interlamellar space for both materials.

Graphical Abstract

Sol-gel process   Co-precipitation from nitrates

M= 25000   2 µm: M= 40000   1 µm:

LDHs with better quality, higher crystallinity, high purity are obtained by sol-gel method
MgAl–LDH: alkoxides + water/NaOH solution at room temperature
CaAl–LDH: alkoxides + $NaNO_3$ solution at room temperature

Highlights

- A novel version of sol–gel synthesis was utilized to prepare two types of layered double hydroxides.
- The platelets have well-defined hexagonal morphology.
- The products have thin crystals with high aspect ratio.

✉ István Pálinkó
palinko@chem.u-szeged

[1] Department of Organic Chemistry, University of Szeged, Dóm tér 8, Szeged H-6720, Hungary

[2] Materials and Solution Structure Research Group, Institute of Chemistry, University of Szeged, Aradi Vértanúk tere 1, Szeged H-6720, Hungary

[3] Department of Applied and Environmental Chemistry, University of Szeged, Rerrich Béla tér 1, Szeged H-6720, Hungary

[4] MTA-SZTE Reaction Kinetics and Surface Chemistry Research Group, Rerrich Béla tér 1, Szeged H-6720, Hungary

[5] Department of Inorganic and Analytical Chemistry, University of Szeged, Dóm tér 7, Szeged H-6720, Hungary

1 Introduction

Layered double hydroxides (LDHs) belong to a family of inorganic clay-type materials with the following general formula: $[M^{2+}_{1-x}M^{3+}_x(OH)_2][A^{n-} \times m~H_2O]$, where M^{2+} and M^{3+} are divalent and trivalent metal ions, respectively [1]. Some representatives with differently-charged cations are also known [2–4]. The materials consist of positively charged layers, compensated by exchangeable, hydrated anions ($A^{n-} \times m~H_2O$) in the interlamellar space [5]. The permanent positive charge of the lamellae is a result of the replacement of a divalent cation in the brucite-like $M(OH)_2$ structure with a trivalent one; each M^{3+} ion adds one extra charge, neutralized by intercalated anions. The high variance of their composition provides multiple applications as catalysts [6], polymer additives [7], adsorbents [8], precursors [9], materials for energy storage and production [10–12], carriers [13, 14], etc. Mostly, they occur as flake-like, irregular grains, although various methods are applied to produce LDHs with exotic morphologies, e.g., wires, toroids, flowers, hollow spheres [15–18]. These unusual shapes are obtained either by template-driven techniques or bi-phase reactions. These materials draw the attention of researchers, since their higher specific surface area may lead to increased efficiency in catalytic applications and water treatment [19, 20]. Let us point out that phase-pure LDHs with symmetrical, high aspect ratio crystals are difficult to synthesize; mainly hydrothermal and urea hydrolysis processes are used for this purpose [21, 22]. Their main disadvantages are as follows: synthesis at high temperature, preferably in an autoclave, and long reaction time.

Sol–gel technique is a convenient and wide-spread method for the synthesis of nanoparticles with high purity and uniform size distribution including titanates, zirconates, and silicates [23]. Few reports have also been published where LDH have been prepared via this method. The preparation of the most common representative material of this family, Mg_2Al–LDH (hydrotalcite) was described first [24], and it is still the focal point of the limited literature amongst a few other examples [25–28]. It was reported that Ca_2Al–LDH (hydrocalumite) was prepared by a sol–gel type method from alkoxide reagents in aqueous medium [29]. An advantage of this synthesis is the simpler waste management due to the lack of organic solvents, used in the vast majority of the sol–gel techniques. However, a garnet material, cubic katoite, a silicate-free hydrogrossular, was also obtained as a by-product.

In this contribution, we communicate a facile, novel synthesis of hydrocalumite and hydrotalcite. The novelty of the method relative to the widely used one is the significant improvement in crystallinity, the more regular hexagonal morphology and milder processing conditions. Furthermore, omitting organic solvents, waste, energy, and synthesis time

is significantly reduced. Our procedure involves mixing and grinding the solid salts followed by their hydrolysis at room temperature. This organic solvent-free method was optimized to produce the ultrapure LDHs.

2 Experimental

2.1 Starting materials

Analytical grade calcium methoxide ($Ca(OMe)_2$), magnesium ethoxide ($Mg(OEt)_2$), aluminium ethoxide ($Al(OEt)_3$), and sodium nitrate ($NaNO_3$) were purchased from Sigma-Aldrich and were used without further purification. Concentrated (~20 M) sodium hydroxide solution was prepared using the solid material (NaOH, ≥99%) purchased from VWR. From the solution, poorly soluble Na_2CO_3 was filtered off, and 3 M stock solutions were diluted when necessary. Water was deionized by reverse osmosis.

2.2 Synthesis

In a typical method, a total of 0.01 mol mixture of 2:1 calcium or magnesium alkoxide and aluminium ethoxide was added to 50 cm³ stirred aqueous medium to undergo a mild reaction. For optimization, a set of solutions were prepared: pure water, a portion of $NaNO_3$ solution of 0.01 mol $NaNO_3$ (equimolar to the metals mimicking the nitrate content of co-precipitation), pH = 13 NaOH solution without $NaNO_3$, a portion of $NaNO_3$ solution with 0.01 mol $NaNO_3$ with pH = 13, set by NaOH. We selected the solutions considering the followings: (i) the classic co-precipitation is performed at pH = 13, (ii) LDHs containing interlamellar NO_3^- ions are favored if ion exchanged is required after synthesis. Also, we compared the materials obtained by sol–gel process with those prepared in our group previously. After a few minutes, white gel was obtained and was stirred for 3 days at room temperature. Post-synthetic ageing was performed at room temperature, 60 °C, and 90 °C for a week. For comparison, the LDHs were prepared by the co-precipitation method described elsewhere [30, 31]. Briefly, nitrate salts of the corresponding metals were dissolved in water, followed by addition of 3 M NaOH solution until pH reaches 13.

The solid substances were separated by filtration, and were washed with water three times, 40 cm³ each and dried at 60 °C overnight.

2.3 Characterization

Powder X-ray diffraction (XRD) patterns of the solid samples were recorded in the $2\theta = 5$–$60°$ range (θ is the incidence angle of the X-ray beam) on a Philips PW1710

instrument with a secondary monochromator, using CuK_α ($\lambda = 0.1542$ nm) radiation with 4°/min scanning step. Phase analysis and data evaluation were performed with XPowder program package and Expo2014 [32] was used for pattern indexing.

Morphological studies were carried out using a Hitachi S-4700 scanning electron microscope (SEM) at various magnifications with 10 kV accelerating voltage after noble metal deposition to the surface.

The Fourier-transform infrared (FT-IR) spectra of the samples were recorded on a JASCO FTIR-4700 spectrometer equipped with a DTGS detector in attenuated total reflectance (ATR) mode. Spectral resolution was $1\,cm^{-1}$ and a total number of 256 scans were collected for a spectrum. The spectra were baseline-corrected and smoothed.

3 Results and discussion

The main goal of our study was to obtain CaAl– and MgAl–LDH via a modified sol–gel method, and compare their physical with those of co-precipitated ones. Thus, synthesis optimization is going to be presented first. For product characterization, primarily powder X-ray diffractometry was applied by assigning the reflections based on the JCPDS database.

3.1 Preparation of CaAl–LDH by sol–gel synthesis

Two products were observed upon the hydrolysis of calcium methoxide and aluminium ethoxide. Katoite (JCPDS No. 24-0217) and hydrocalumite were simultaneously generated. However, the excess amount of katoite obtained in the reaction with pure water could be reduced with equimolar (to the metal ions) $NaNO_3$ dissolved. In fact, with no ageing introduced, only the nitrate form of hydrocalumite (JCPDS No. 89-6723) is observable on the X-ray diffractogram, while after weeklong treatments at 60 and 90 °C, the garnet is detectable in small and large quantities, respectively (Fig. 1) meaning that the formation of katoite has a kinetic barrier at lower temperature.

In parallel, the average particle thickness grows (as FWHM of $00l$ reflections shrinks), and the ratios of $00l$ reflections to other ones rise. Such change can be attributed to different morphological properties, since the quantity of given lattice planes is in correlation with reflection intensities [33, 34]. A preset pH value of 13 results in two impacts: (i) dissolution of airborne CO_2 and formation of carbonate-intercalated hydrocalumite (JCPDS No. 41-0219) and (ii) preferential production of katoite. Both are amplified with increased ageing temperature. A mixed solution of NaOH and $NaNO_3$ reduces the quantity of $CaAl(CO_3)$–
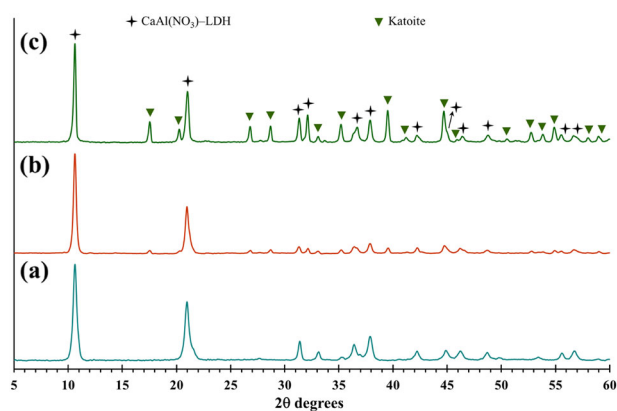

Fig. 1 XRD patterns of hydrocalumite samples obtained by the sol–gel method using $NaNO_3$ solution with **a** no ageing and weeklong ageing at **b** 60 °C or **c** 90 °C
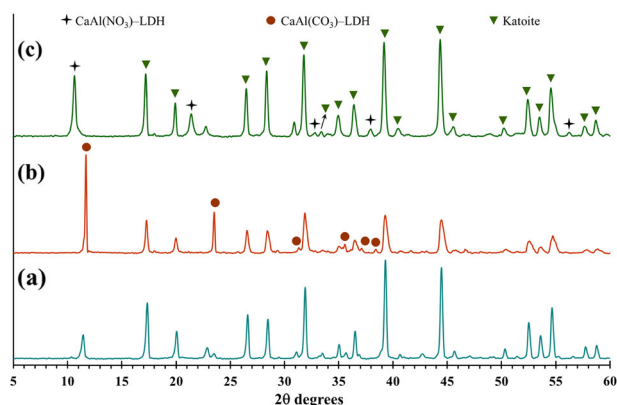

Fig. 2 XRD patterns of hydrocalumites obtained by the sol–gel method without ageing using **a** water, **b** 0.1 M NaOH solution, and **c** NaOH–$NaNO_3$ mixed solution

LDH in the product, but katoite is still present after ageing. The same tendencies apply for the synthesis carried out in pure water (Fig. 2).

XRD reflection assignation was performed on pure CaAl(NO_3)–LDH as well as mixed sample of katoite and CaAl(CO_3)–LDH for all materials (Fig. 3).

3.2 Preparation of MgAl–LDH by sol–gel synthesis

Production of hydrotalcite is hindered by the usage of nitrate-containing solutions (metal hydroxides were formed, Fig. 4). The reflections of magnesium hydroxide and aluminium hydroxide were assigned using JCPDS No. 84-2164 and JCPDS No. 83-2256 (bayerite form), respectively.

However, MgAl–LDH was formed using water or 0.1 M aqueous NaOH solution as the hydrolysis medium. Exactly the opposite conditions were required to get hydrocalumite than hydrotalcite (Fig. 5).
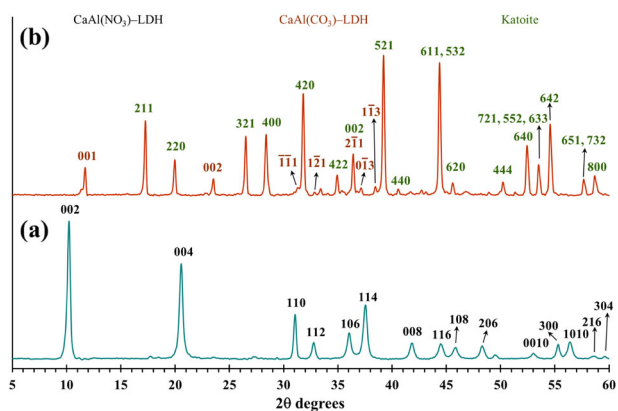
Fig. 3 Miller indices on PXRD pattern of **a** CaAl(NO$_3$)–LDH and **b** CaAl(CO$_3$)–LDH and katoite

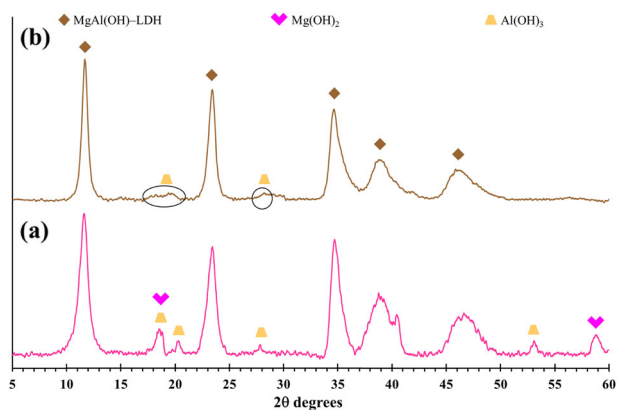Fig. 4 XRD pattern of hydrotalcites obtained by the sol–gel method without ageing using **a** NaNO$_3$ solution and **b** NaOH–NaNO$_3$ mixed solution
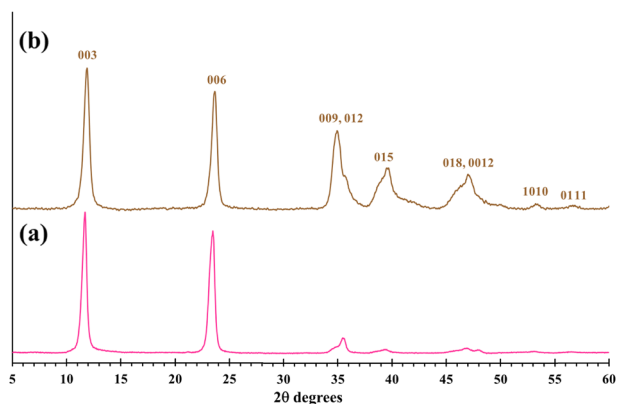

Fig. 5 XRD pattern and Miller indices of hydrotalcites obtained by sol–gel method without ageing using **a** water and **b** 0.1 M NaOH solution

The main product of these sol–gel syntheses is either hydroxide or carbonate (airborne) intercalated MgAl–LDH. Although their XRD patterns (JCPDS Nos. 35-0964 and

Fig. 6 IR spectrum of sol–gel hydrocalumite obtained with NaNO$_3$ solution

70-2151) are nearly identical, our material is identified as the hydroxide form (from the measured basal spacing), and its indices are shown in Fig. 5, although probably a tiny amount of CO$_3^{2-}$ ions are present in the product.

Both the chemical composition and physical properties are unaffected by thermal treatment. IR spectra were recorded of the LDHs produced by sol–gel method to observe if any organic material was incorporated into the LDHs. As no sharp absorption band was registered in the region of C–H stretching vibrations (near 3000 cm^{-1}), we conclude that no alcohol or alkoxide is present in detectable amounts. The characteristic band of O–H stretching vibrations, the scissoring vibration of H$_2$O molecules and the intensive stretching band of CO$_3^{2-}$ (absorbed from air) or intercalated NO$_3^-$ are well-distinguished. The IR spectrum of hydrocalumite is shown in Fig. 6, where two types of O–H vibration is separable: OH groups in hydrogen-bonded network are detected in the lower wavenumber region, while isolated OH groups have bands near 3650 cm^{-1}. The appearance of these bands is typical for hydrocalumite, but not for hydrotalcite.

Comparing our results with those presented by Velente et al. [35] upon synthetizing hydrotalcite with the classic sol–gel method, alcohols used as solvents are incorporated in the product, proved by XRD and IR spectroscopy. During the reaction described in this paper, the amount of organics is negligible to water or the anions, thus the LDHs do not contain methanol or ethanol.

3.3 Size and structure of the particles

While the position of the first XRD reflection is in relation with basal spacing (c_0 from Bragg's law and from Expo2014), its FWHM value corresponds to particle thickness (D from Scherrer's equation). The polytype of CaAl(NO$_3$)–LDH is 2H and 3R of MgAl(OH)–LDH, thus their c lattice parameter is $2c_0$ and $3c_0$, respectively.

Stacking the layers results in increment of D, in fact, the average number of piled unit cells (N) and layers in one crystal (N_L) is obtained by division. All values are summarized in Table 1. It should be remarked that preferred orientation should also be under consideration when plate-like crystals are produced. This effect can also be a factor when comparing peak ratios and a small deviation of D parameter is plausible.

The values show that for hydrocalumite the difference in D is small between the sol–gel synthetized and the co-precipitated LDHs, but is roughly tripled for the hydrotalcite samples. The particle sizes are reversed: the diameter of the hydrocalumite particles is multiplied on the sol–gel synthesis for CaAl–LDH, while for the sol–gel synthesized hydrotalcite samples the particle size remained the same. In other words, the aspect ratio for hydrotalcite is unaltered, while it is huge for hydrocalumite. As the particle diameter increases, considering the nearly constant thickness, the lattice planes perpendicular to the direction of growth (i.e., 00l faces) undergo significant rise in the surface area. Since the intensities of the reflections in the pattern correlate with the area of the diffracting face, there is a drastic change in the characteristics of sol–gel sample pattern. Each reflection is observable, but the relative intensities of 00l planes are predominant, while other reflections decay. Similar differences are observed for the hydrotalcite sample as well. Although this LDH has smaller particle size than that of the hydrocalumite sample, a few differences could be observed: the largest crystals grew on using only water for hydrolysis and the smallest ones were developed during co-precipitation. Despite that thickening of the particle has a reverse effect on intensities, the intensities of the reflections

increased meaning the lateral increase had more important effect on the pattern.

3.4 Morphological properties

As it was mentioned before, both LDHs underwent certain changes due to the introduction of the modified sol–gel synthetic method. The peculiarities, anticipated from XRD data are reinforced by the images.

Crystal of co-precipitated hydrocalumite tends to from slabs with hexagonal morphology without sharp edges, typically with diameters somewhat smaller than 1 μm (Fig. 7a). However, on using the sol–gel method of synthesis, large, highly symmetric crystals with sharp edges were formed (Fig. 7b).

SEM micrographs of the hydrotalcite samples are shown in Fig. 8. The thick particles of co-precipitation (Fig. 8a) changed to ordered thin, plate-like crystallites of the sol–gel process (Fig. 8b).

Differences may be attributed to the fact that the polycondensation-type hydrolysis of alkoxides is slower compared to direct hydroxide formation from nitrate salts, but also the positive effect (improved crystallinity, in general) of organic molecules on crystallinity was observed before [36, 37]. Furthermore, the structure of the alkoxides used is isomorphic with that of brucite. Thus, the formation of the LDH layers is a substitution of the alcoholate ions to hydroxide ions, while the totally dissociating nitrate salts suffer a higher degree of structural changes to form the brucite-like lamellae.

3.5 Synthesis of co-precipitated hydrotalcite and hydrocalumite at elevated temperatures

It should be mentioned that high-temperature ageing of the as-prepared LDHs also improves the crystallinity, however, for hydrotalcite, morphology is the same as without ageing. Regarding hydrocalumite, the diameter of the crystals grows, but surface roughness is observable, and less symmetrical plates are obtained. At 90 °C, partial degradation occurs as $Ca(OH)_2$ (JCPDS No. 84-1275) and $Al(OH)_3$ (bayerite form, JCPDS No. 83-2256) are identified on the

Table 1 Crystallographic data of co-precipitated and sol–gel LDHs

LDH	c_0 (nm)	c (nm)	D (nm)	N	N_L
CaAl–LDH co-precipitation	0.856	1.712	30	17.5	35
MgAl–LDH co-precipitation	0.758	2.174	6	3	9
CaAl–LDH sol–gel	0.847	1.694	33	18.5	37
MgAl–LDH sol–gel	0.750	2.150	20	9	27

Fig. 7 SEM micrograph of CaAl (NO$_3$)–LDH obtained by **a** co-precipitation and **b** the sol–gel method
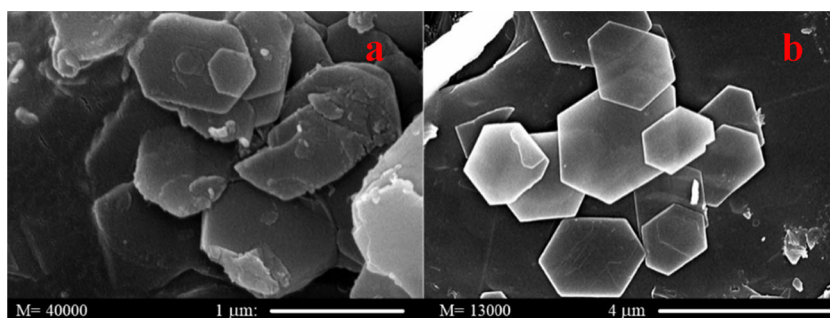
Fig. 8 SEM micrograph of MgAl(OH)–LDH obtained by **a** co-precipitation and **b** the sol–gel method
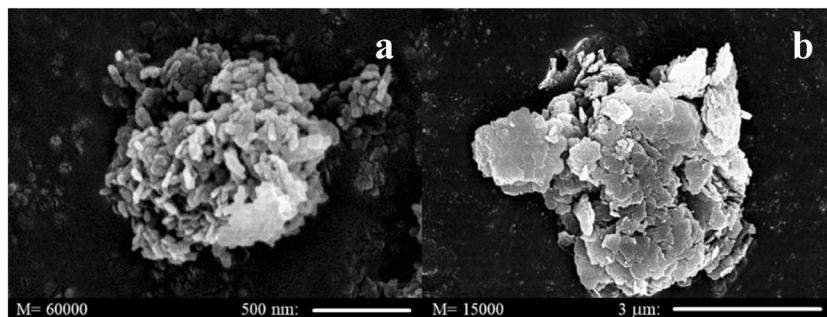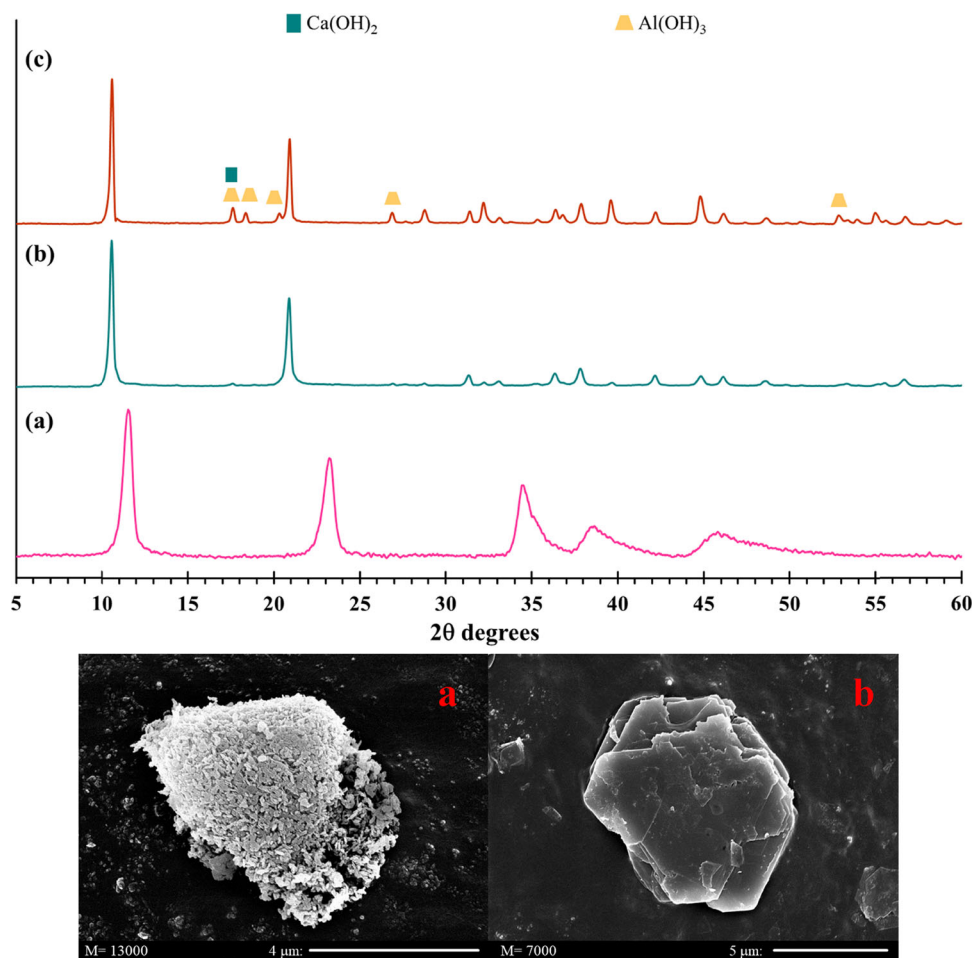

Fig. 9 Upper: XRD pattern of **a** hydrotalcite obtained by co-precipitation and weeklong ageing at 60 °C, **b** hydrocalumite obtained by co-precipitation and weeklong ageing at 60 °C and **c** at 90 °C. Lower: SEM micrographs corresponding to materials **a** and **b**

XRD pattern (Fig. 9). The properties of hydrotalcite are identical after treatment at both temperatures. Altogether, one can declare that the improvement in the quality of the products drawn by sol–gel method is significant, especially with no high temperatures introduced in the latter process.

4 Conclusions

The syntheses of pure hydrocalumite and hydrotalcite were performed by a modified sol–gel type technique. It was found that the presence of nitrate ions and the lack of ageing were required to form pure hydrocalumite; higher ageing temperature favored the formation of katoite garnet, a by-product. On the other hand, nitrate solutions led to the formation of magnesium hydroxide and aluminium hydroxide from precursors to hydrotalcite. The optimal synthesis of this material proceeded in pure water, but aqueous NaOH solution (with pH = 13) as the hydrolytic medium can also be used. Under these conditions, powders with highly crystalline and regular particles with hexagonal morphology were formed with high aspect ratios from both LDHs. The

products described are phase pure, i.e., no other crystalline products (by-products) were obtained. Not using organic solvents in the method developed implies greener reaction conditions, i.e., by using only water as synthesis medium, an environmentally more benign version of the classical sol–gel process has been developed.

Compliance with ethical standards

Conflict of interest The authors declare that they have no conflict of interest.

References

1. Evans DG, Slade RCT (2006) Structural aspects of layered double hydroxides. Struct Bond 119:1–87
2. Thiel JP, Chiang CK, Poeppelmeier KR (1993) Structure of $LiA_{12}(OH)_7 \cdot 2H_2O$. Chem Mater 5:297–304
3. Al Jaafaari AI (2010) Controlling the morphology of nano-hybrid materials. Am J Appl Sci 7:171–177
4. Mostafa MS, Bakr AA, El Naggar AMA, Sultan EA (2016) Water decontamination via the removal of Pb(II) using a new generation of highly energetic surface nano-material: $Co^{+2}Mo^{+6}$ LDH. J Colloid Interface Sci 461:261–272
5. Khan AI, O'Hare D (2002) Intercalation chemistry of layered double hydroxides: recent developments and applications. J Mater Chem 12:3191–3198
6. Xu ZP, Zhang J, Adebajo MO, Zhang H, Zhou C (2011) Catalytic applications of layered double hydroxides and derivatives. Appl Clay Sci 53:139–150
7. Purohit PJ, Wang D, Wurm A, Schick C, Schönhals A (2014) Comparison of thermal and dielectric spectroscopy for nanocomposites based on polypropylene and layered double hydroxide—proof of interfaces. Eur Polym J 55:48–56
8. Goha K, Lima T, Dong Z (2008) Application of layered double hydroxides for removal of oxyanions: a review. Water Res 42:1343–1368
9. Tichit D, Gérardin C, Durand R, Coq B (2006) Layered double hydroxides: precursors for multifunctional catalysts. Top Catal 39:89–96
10. Ahmed N, Morikawa M, Izumi Y (2012) Photocatalytic conversion of carbon dioxide into methanol using optimized layered double hydroxide catalysts. Catal Today 185:263–269
11. Fan K, Chen H, Ji Y, Huang H, Claesson PM, Daniel Q, Philippe B, Rensmo H, Li F, Luo Y, Sun L (2016) Nickel–vanadium monolayer double hydroxide for efficient electrochemical water oxidation. Nat Commun 7:11981
12. Jagadale AD, Guan G, Li X, Du X, Ma X, Hao X, Abudula A (2016) Ultrathin nanoflakes of cobalt–manganese layered double hydroxide with high reversibility for asymmetric supercapacitor. J Power Sources 306:526–534
13. Del Hoyo C (2007) Layered double hydroxides and human health: an overview. Appl Clay Sci 36:103–121
14. Cornejo J, Celis R, Pavlovic I, Ulibarri MA (2008) Interactions of pesticides with clays and layered double hydroxides: a review. Clay Miner 43:155–175

15. Hu G, O'Hare D (2005) Unique layered double hydroxide morphologies using reverse microemulsion synthesis. J Am Chem Soc 127:17808–17813
16. Ni X, Kuang K, Jin X, Xiao X, Liao G (2010) Large scale synthesis of porous microspheres of Mg–Al-layerd double hydroxide with improved fire suppression effectiveness. Solid State Sci 12:546–551
17. Wu H, Jiao Q, Zhao Y, Huang S, Li X, Liu H, Zhou M (2010) Synthesis of Zn/Co/Fe-layered double hydroxide nanowires with controllable morphology in a water-in-oil microemulsion. Mater Charact 61:227–232
18. Tao Y, Ruiyi L, Tingting Y, Zaijun L (2015) Nickel/cobalt layered double hydroxide hollow microspheres with hydrangea-like morphology for high-performance supercapacitors. Electrochim Acta 152:530–537
19. Yang M, Liu J, Chang Z, Williams GR, O'Hare D, Zheng X, Sun X, Duan X (2011) $Mg/Al-CO_3$ layered double hydroxide nanorings. J Mater Chem 20:14741–14746
20. Chen L, Li C, Wei Y, Zhou G, Pan A, Wei W, Huang B (2016) Hollow LDH nanowires as excellent adsorbents for organic dye. J Alloy Compd 687:499–505
21. Francois M, Renaudin G, Evrard O (1998) A cementitious compound with composition $3CaO \cdot Al_2O_3 \cdot CaCO_3 \cdot 11H_2O$. Acta Crystallogr C 54:1214–1217
22. Ogawa M, Kaiho H (2002) Homogeneous precipitation of uniform hydrotalcite particles. Langmuir 18:4240–4242
23. Wen J, Wilkes GL (1996) Organic/inorganic hybrid network materials by the sol–gel approach. Chem Mater 8:1667–1681
24. Lopez T, Bosch P, Ramos E, Gomez R, Novaro O, Acosta D, Figueras F (1996) Synthesis and characterization of sol–gel hydrotalcites. Structure and texture. Langmuir 12:189–192
25. Prinetto F, Ghiotti G, Graffin P, Tichit D (2000) Synthesis and characterization of sol–gel Mg/Al and Ni/Al layered double hydroxides and comparison with co-precipitated samples. Microporous Mesoporous Mater 39:229–247
26. Aramendía MA, Borau V, Jiménez C, Marinas JM, Ruiz JR, Urbano FJ (2002) Comparative study of Mg/M(III) (M = Al, Ga, In) layered double hydroxides obtained by coprecipitation and the sol–gel method. J Solid State Chem 168:156–161
27. Yamaguchi N, Ando D, Tadanaga K, Tatsumisago M (2007) Direct formation of Mg–Al-layered double-hydroxide films on glass substrate by the sol–gel method with hot water treatment. J Am Ceram Soc 90:1940–1942
28. Tadanaga K, Miyata A, Ando D, Yamaguchi N, Tatsumisago M (2012) Preparation of Co–Al and Ni–Al layered double hydroxide thin films by a sol–gel process with hot water treatment. J Sol-Gel Sci Technol 62:111–116
29. Cota I, Ramírez E, Medina F, Sueirad JE, Layrac G, Tichit D (2010) New synthesis route of hydrocalumite-type materials and their application as basic catalysts for aldol condensation. Appl Clay Sci 50:498–502
30. Varga G, Kukovecz Á, Kónya Z, Korecz L, Muráth S, Csendes Z, Peintler G, Carlson S, Sipos P, Pálinkó I (2016) Mn(II)–amino acid complexes intercalated in CaAl-layered double hydroxide—well-characterized, highly efficient, recyclable oxidation catalysts J Catal 335:125–134
31. Muráth S, Somosi Z, Tóth IY, Tombácz E, Sipos P, Pálinkó I (2017) Delaminating and restacking MgAl-layered double hydroxide monitored and characterized by a range of instrumental methods. J Mol Struct 1140:77–82
32. Altomare A, Cuocci C, Giacovazzo C, Moliterni A, Rizzi R, Corriero N, Falcicchio A (2013) *EXPO2013*: a kit of tools for phasing crystal structures from powder data. J Appl Crystallogr 46:1231–1235

33. Scardi P, Leoni M (2001) Diffraction line profiles from poly-disperse crystalline systems. Acta Crystallogr A 57:604–613

34. Inoue M, Hirasawa I (2013) The relationship between crystal morphology and XRD peak intensity on $CaSO_4 \cdot 2H_2O$. J Cryst Growth 380:169–175

35. Valente JS, Cantú MS, Cortez JGH, Montiel R, Bokhimi X, López-Salinas E (2006) Preparation and characterization of sol–gel MgAl hydrotalcites with nanocapsular morphology. J Phys Chem C 111:642–651

36. Yang M, McDermott O, Buffet J-C, O'Hare D (2014) Synthesis and characterisation of layered double hydroxide dispersions in organic solvents. RSC Adv 4:51676–51682

37. Wang J, Wei Y, Yu J (2013) Influences of polyhydric alcohol co-solvents on the hydration and thermal stability of MgAl–LDH obtained via hydrothermal synthesis. Appl Clay Sci 72:37–43